

Gaze-Based Task Decomposition for Robot Manipulation in Imitation Learning

Ryo Takizawa^{*1}, Yoshiyuki Ohmura¹, Yasuo Kuniyoshi¹

Abstract—In imitation learning for robotic manipulation, decomposing object manipulation tasks into multiple sub-tasks is essential. This decomposition enables the reuse of learned skills in varying contexts and the combination of acquired skills to perform novel tasks, rather than merely replicating demonstrated motions. Gaze plays a critical role in human object manipulation, where it is strongly correlated with hand movements. We hypothesize that an imitating agent’s gaze control—fixating on specific landmarks and transitioning between them—simultaneously segments demonstrated manipulations into sub-tasks. In this study, we propose a simple yet robust task decomposition method based on gaze transitions. The method leverages teleoperation, a common modality in robotic manipulation for collecting demonstrations, in which a human operator’s gaze is measured and used for task decomposition as a substitute for an imitating agent’s gaze. Notably, our method achieves consistent task decomposition across all demonstrations for each task, which is desirable in contexts such as machine learning. We applied this method to demonstrations of various tasks and evaluated the characteristics and consistency of the resulting sub-tasks. Furthermore, through extensive testing across a wide range of hyperparameter variations, we demonstrated that the proposed method possesses the robustness necessary for application to different robotic systems.

I. INTRODUCTION

Imitation stands as a uniquely promising approach for enabling robots to function as autonomous agents capable of acquiring object manipulation skills that align with human intentions. Here, the ability for an imitating agent to automatically decompose a demonstrated manipulation into multiple sub-tasks is instrumental for executing long-horizon tasks and for reusing or combining learned skills.

In this context, a method is required that can segment demonstrations of various tasks into sub-tasks without the need for additional training or diverse data collection. In addition, recent imitation learning methods based on deep learning typically require hundreds of demonstrations for each task, and it is desirable to consistently decompose all of these demonstrations into the same set of sub-tasks. However, few methods have been proposed for such task decomposition, and none of them are able to perform it in a consistent manner. As a result, demonstrations are often manually segmented into sub-tasks [1], otherwise the goal state, which conditions a policy model, is usually substituted with a state a certain number of steps ahead [2], [3].

¹Laboratory for Intelligent Systems and Informatics, Graduate School of Information Science and Technology, The University of Tokyo, 7-3-1 Hongo, Bunkyo-ku, Tokyo, Japan (Email: {takizawa, ohmura, kuniyoshi}@isi.imi.i.u-tokyo.ac.jp)

^{*}Corresponding Author

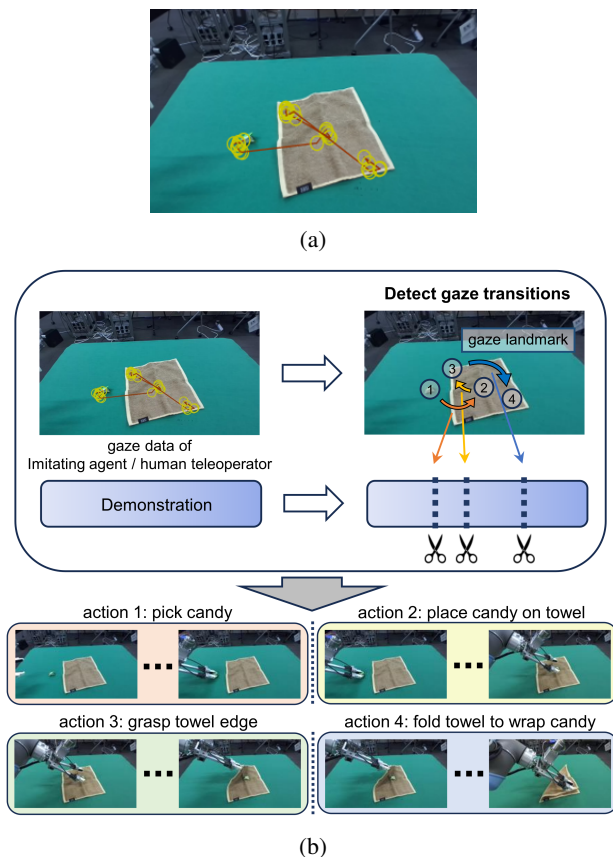


Fig. 1: Gaze itself possesses an inherent structure in object manipulation, which enables task decomposition by detecting transitions between gaze landmarks during demonstration. (a) Gaze transition of a human teleoperating a robot. (b) Overview of our proposed method.

In this study, we focus on gaze information to achieve consistent task decomposition without the need for additional training or diverse data collection. As Yarbus stated, “Eye movement reflects the human thought processes; so the observer’s thought may be followed to some extent from records of eye movement” [4], suggesting that gaze is a naturally evolved tool for understanding ongoing events. In particular, it is well established that during human object manipulations, individuals repeatedly fixate their gaze on task-relevant landmarks for certain periods and then move on to the next (Fig. 1a), and that these gaze transition behaviors are tightly coupled with the motor planning processes of hands [5], [6], [7]. These insights suggest that leveraging an imitating agent’s gaze information, including its position

and associated visual features, provides a pathway for task decomposition in demonstrated object manipulations.

In this paper, we show that a simple approach of detecting transitions between gaze landmarks during imitation enables robust and consistent task decomposition of demonstrations (Fig. 1b). In the current imitation learning framework, it is common to collect demonstrations via human teleoperation. Several approaches have been proposed that simultaneously measure the teleoperator’s gaze alongside motion recording and use it as a substitute for an imitating agent’s gaze. [8], [9]. These methods improved both the robustness and dexterity of the imitated actions with minimal modifications to the conventional teleoperation system. Similar to these methods, we record the teleoperator’s gaze information (Fig. 1a) and use it for task decomposition. Our proposed method segments demonstrations at the operator’s gaze transition timings, identified using a threshold-based approach that detects abrupt changes in gaze position and visual features around the gaze point. To ensure consistent task decomposition across all demonstrations of the same task, we also develop a refinement process that automatically adjusts these thresholds for each demonstration.

We apply our method to demonstration datasets of three tasks collected for imitation learning and evaluated the characteristics and consistency of the resulting sub-tasks. Furthermore, we investigate how the proposed refinement process improves the consistency of task decomposition and the robustness to variations in hyperparameters.

II. RELATED WORK

A. Robot Manipulation Imitation Using Task Decomposition

Many approaches have been proposed that utilize temporal task decomposition for imitation learning in robot manipulation. A common strategy for enhancing robustness in long-horizon tasks is to employ goal-conditioned policy models [1], [2]. In these methods, the task is decomposed into multiple sub-tasks, and the goal states of each sub-task are conditioned to the model stepwise. Furthermore, recent years have seen an increase in language-conditioned models aimed at multi-task capabilities [10], [11], [12], [13]. In datasets for language-conditioned models, sub-task-level instructions, such as “pick an apple” and “place on a plate”, are generally preferred over task-level instructions, such as “move an apple to a plate” [14]. These goal- or language-conditioned methods implicitly assume that object manipulations in the given demonstrations are segmented into individual sub-tasks. However, in most existing work, the segmentation of these demonstrations is performed manually. In this context, our proposed method can reduce annotation costs by automating part of the data collection process, specifically by segmenting demonstrations.

B. Conventional Task Decomposition Methods

In the field of *Action Segmentation*, numerous methods have been proposed for the temporal segmentation of actions and motions involving object manipulation [15], [16], [17], [18], [19], [20], [21], including ones using human gaze

information [22], [23]. However, most of these methods are primarily designed for human action recognition, and very few are suitable for task decomposition of robotic object manipulation. Moreover, because many of these approaches rely heavily on visual, data-driven techniques, applying them to a wide variety of robotic hardware requires the construction of new datasets tailored to each specific platform.

Although research on task decomposition in robotic object manipulation is limited, several studies have been proposed. Liang et al. optimize the transitions between the manipulating (*tool*) and the manipulated (*target*) objects, using these transition points to segment tasks; however, their method requires the 6D poses of all relevant objects [24]. In contrast, our proposed method does not require explicit modeling of the environment. Lee et al. reduce the dimensionality of whole-body trajectories using PCA and further model them with GMM, assigning each Gaussian component to a sub-task [25]. In contrast, our method does not utilize hand motion data, making it robust to variations in such movements. Zhu et al. employ neural networks (NNs) for latent-space clustering to achieve task decomposition; however, their approach requires training the NN for new tasks, and the number of sub-tasks is determined solely by the time step length of each segment [26]. In contrast, our method does not require training of NNs, thus enabling high-speed processing, and it determines the number of sub-tasks based on the number of gaze transitions, thus ensuring higher generality. Zhang et al. utilize latent vectors derived from pre-trained models specialized for object manipulation, such as R3M [27], and perform task decomposition based on the distances between these latent vectors [28]. Similar to our method, their approach employs detection-based task decomposition without requiring additional data or training. However, compared to distance metrics in latent vector space, gaze transitions have been extensively studied for their coordination with hand movement planning in object manipulation, indicating that gaze-based task decomposition offers greater reliability.

III. METHOD

In this section, we first formulate the task decomposition of object manipulation based on gaze transitions. We then detail our implementation procedure. Specifically, we begin by explaining how gaze transitions are detected from time-series gaze data, and subsequently describe the refinement process used to achieve consistent decomposition across the demonstration dataset.

A. Gaze-based Task Decomposition

We consider a scenario in which a human remotely controls a robot using only visual information to collect demonstrations of object manipulation for imitation learning. Multiple demonstrations (typically ranging from several tens to hundreds) are collected for each task, and all demonstrations of the same task share an identical set of sub-tasks. Let $\{g_t\}_{t=0}^T$ denote the time-series of the human teleoperator’s gaze positions, and $\{f_t\}_{t=0}^T$ the time-series

of the visual features observed around those gaze positions. When the demonstrated task is decomposed into a set of sub-tasks $\{\tau_k\}_{k=0}^K$, the objective in this section is to determine the $K - 1$ time steps at which the sub-tasks switch (i.e. $\{t \mid k(t + 1) = k(t) + 1\}$), using the gaze information $\{g_t\}$ and $\{f_t\}$.

In human object manipulation, it is well-established that each task has a specific set of gaze landmarks $\{l_i\}_{i=0}^N$, and that humans fix their gaze on each landmark for a certain duration, then sequentially transition to the next landmark [6], [7], [5]. Here, the landmark index i is arranged according to the order in which landmarks are fixated from the start of the task (duplicates may occur).

In this study, we hypothesize that the time steps at which the index of the fixated gaze landmark changes, $\{t \mid i(t + 1) = i(t) + 1\}$, correspond to the time steps at which the sub-tasks switch, $\{t \mid k(t + 1) = k(t) + 1\}$. In other words, we realize task decomposition by detecting transitions of gaze landmarks.

Let $p_t^{i(t)}$ be the location of the landmark $c_{i(t)}$ in the teleoperator’s field of view at time step t . Then, the gaze position g_t and the visual feature f_t at that gaze position can be written as follows:

$$g_t = p_t^{i(t)} + \epsilon_t, \quad (1)$$

$$f_t = f(g_t) + \zeta_t = f(p_t^{i(t)} + \epsilon_t) + \zeta_t, \quad (2)$$

where ϵ_t and ζ_t represent noise in the gaze position and perturbations in the visual features caused, for example, by the end-effector movements, respectively, and $f(\cdot)$ is the visual feature extractor at the given gaze position.

In other words, by leveraging the relationships in Eqs. 1 and 2, we can detect the transitions of gaze landmarks $\{l_i\}$ from the gaze information $\{g_t\}$ and $\{f_t\}$, and thereby achieve task decomposition of the demonstrated object manipulation.

B. Gaze Transition Detection

We now describe the implementation details for segmenting demonstrations based on gaze transitions. As discussed in the previous section, an algorithm for detecting the time steps at which gaze landmarks switch, using time-series gaze data, is critical for the task decomposition.

1) *Median Filtering*: Gaze data typically contain noise. Even when the teleoperator is fixating on a stationary gaze landmark, the recorded gaze positions often exhibit fluctuations. Moreover, the teleoperator may occasionally shift its gaze for a short period to a different landmark during object manipulation. To handle such noise in a simple yet effective manner, we adopt a median-filtering approach. Specifically, for the teleoperator’s gaze position g_t , we apply the process shown in Eq. 3 with a window size w as a hyperparameter, and use the filtered gaze data \hat{g}_t in all subsequent processing:

$$\hat{g}_t = \text{median}(g_{t-\frac{w}{2}:t+\frac{w}{2}}). \quad (3)$$

2) *Visual Features Around the Gaze*: Gaze transitions cause not only positional changes in the gaze but also variations in the visual features around the gaze. We also consider detecting gaze transitions using visual features. To robustly detect changes in visual features, it is essential to employ a feature extractor based on high-quality representation learning. For each time step, we crop an $b \times b$ region centered at the filtered gaze position \hat{g}_t from both the left and right images and feed these cropped images into the pre-trained CLIP model [29] to extract their feature vectors $f_t \in \mathbb{R}^{512 \times 2}$. This time-series of feature vectors, along with the gaze position, is used for gaze transition detection in this study.

3) *Change Detection*: For the obtained gaze position \hat{g}_t and visual feature f_t , we compute the difference from the previous time step to detect abrupt changes in the time-series data caused by gaze transitions:

$$s_t^{pos} = \|\hat{g}_t - \hat{g}_{t-1}\|, \quad (4)$$

$$s_t^{feat} = -\frac{\log(f_{t-1}^{leftT} f_t^{left} + 1) + \log(f_{t-1}^{rightT} f_t^{right} + 1)}{2} + \log 2, \quad (5)$$

where s_t^{pos} and s_t^{feat} represent the change scores for the gaze position and the visual features, respectively. Specifically, s_t^{pos} is the Euclidean distance between the two 4-dimensional vectors representing the left and right gaze positions. Meanwhile, s_t^{feat} is derived from the inner products between the corresponding gaze feature vectors in consecutive time steps, normalized to ensure non-negativity, and then averaged for the left and right features.

We introduce the thresholds θ_{pos} and θ_{feat} as hyperparameters for these two change scores, and identify any time step at which both change scores exceed their respective thresholds as a change point $c_i \in C$.

C. Refinement Based on Decomposition Consistency

In recent machine learning–based imitation learning methods, particularly those relying on multiple demonstrations, all demonstrations of the same task typically comprise a consistent set of sub-tasks. In such scenarios, it becomes possible to further improve the consistency of task decomposition across all these demonstrations. Here, we introduce a refinement procedure, $C \rightarrow C^*$, to ensure that all demonstrations of the same task share as consistent a number of sub-tasks as possible. The algorithm for this process is summarized in Algorithm 1.

First, we enumerate the number of change points $|C|$ obtained via the gaze transition detection (Section III-B) for every demonstration and denote the most frequent value by s . We assume s to be the number of sub-tasks for the task and adjust the thresholds θ_{pos} and θ_{feat} so that the number of segments in each demonstration matches s . Specifically, for any demonstration whose segmented count is smaller than s , we reduce both thresholds by 1% at each iteration;

Algorithm 1 Task Decomposition Refinement Process

Given: A set of demonstrations for the same task:

$$D = \{(s_t^{\text{pos}}, s_t^{\text{feat}})^{(n)}\}_{n=1}^N, \quad t \in [0, T^{(n)}],$$

where N is the number of demonstrations and $T^{(n)}$ is the total time steps in the n -th demonstration.

Notation: Let the function $\text{detect}(\cdot)$ perform change point detection:

$$C \leftarrow \text{detect}(\{s_t^{\text{pos}}\}, \{s_t^{\text{feat}}\}, \theta_{\text{pos}}, \theta_{\text{feat}}).$$

Initialize: $\theta_{\text{pos}}, \theta_{\text{feat}} \leftarrow$ default values

```
1: for  $n = 1$  to  $N$  do
2:    $C^{(n)} \leftarrow \text{detect}(\{s_t^{\text{pos}}\}^{(n)}, \{s_t^{\text{feat}}\}^{(n)}, \theta_{\text{pos}}, \theta_{\text{feat}})$ 
3: end for
4:  $s \leftarrow \text{mode}(\{|C^{(n)}|\}_{n=1}^N)$ 
5: for  $n = 1$  to  $N$  do
6:   while  $|C^{(n)}| < s$  do
7:      $\theta_{\text{pos}}, \theta_{\text{feat}} \leftarrow 0.99\theta_{\text{pos}}, 0.99\theta_{\text{feat}}$ 
8:      $C^{(n)} \leftarrow \text{detect}(\{s_t^{\text{pos}}\}^{(n)}, \{s_t^{\text{feat}}\}^{(n)}, \theta_{\text{pos}}, \theta_{\text{feat}})$ 
9:   end while
10:  while  $|C^{(n)}| > s$  do
11:     $\theta_{\text{pos}}, \theta_{\text{feat}} \leftarrow 1.01\theta_{\text{pos}}, 1.01\theta_{\text{feat}}$ 
12:     $C^{(n)} \leftarrow \text{detect}(\{s_t^{\text{pos}}\}^{(n)}, \{s_t^{\text{feat}}\}^{(n)}, \theta_{\text{pos}}, \theta_{\text{feat}})$ 
13:  end while
14:   $C^{*(n)} \leftarrow C^{(n)}$ 
15: end for
Return:  $\{C^{*(n)}\}_{n=1}^N$ 
```

conversely, for a count larger than s , we increase them by 1%. If no threshold values are found that yield s segments within a maximum number of iterations, that demonstration is treated as a detection failure and excluded from the training data.

Finally, the refined set of change points C^* obtained by this process is taken as the sub-task boundary for each demonstration, enabling us to divide as many demonstrations as possible into a consistent number of sub-tasks.

IV. EXPERIMENTS

A. Robot System

We used a dual-arm robotic system that was previously developed for imitation learning through teleoperation [8]. A human teleoperator controlled the robot remotely by viewing its environment through a head-mounted display (HMD), which simultaneously recorded the operator’s eye gaze. The system can be configured to use either a physical dual-arm robot, a pair of UR5 robots from Universal Robots Inc., or a simulated counterpart, enabling the collection of expert demonstrations in both real and virtual settings [30]. The recorded gaze data were provided as pixel coordinates corresponding to the images displayed on the HMD.

In this study, we evaluated our task decomposition method using an expert demonstration dataset collected through this system. Each demonstration included synchronized left and

right image streams, along with corresponding gaze data, and all of these were employed in our experiments.

B. Task Setup

We evaluated the proposed methods on three object manipulation tasks, two conducted using the physical robot system and one within a simulated environment.

We first collected approximately 100 demonstrations for each task as follows:

- **WrapCandy (real robot, 64 demos):** In this task, a green candy and a brown handkerchief are arranged on a table with a green tablecloth. The position and orientation of the two objects are randomized on the table. The robot grasps the candy and place it in the middle of the handkerchief. The robot then picks up the (top) left corner of the handkerchief and folds it to wrap the candy.
- **PenInCup (real robot, 125 demos):** In this task, a blue marker pen and a red cup are placed on a table; the position and orientation of the two objects is randomized on the table. The robot picks up the pen and puts it in the cup.
- **PileBox (simulated robot, 147 demos):** In this task, red and blue boxes are placed on a wooden table; the position and orientation of the two boxes is randomized. The robot grabs the red box and places it on top of the green box.

C. Task Decomposition Results

For each task, we performed task decomposition on all demonstrations in the dataset. In doing so, we used the same hyperparameters across all demonstrations and tasks: $w = 20, b = 256$ (overall image size: 1280×720), $\theta_{\text{pos}} = 50, \theta_{\text{feat}} = 0.05$. Fig. 2 presents a representative example of segmentation results for each task.

In the WrapCandy task, the series of object manipulations was segmented into four actions: (1) picking up the candy, (2) placing the candy at the center of the towel, (3) grasping the upper-left corner of the towel, and (4) folding the towel. In the PenInCup task, the demonstration was segmented into two actions: (1) picking up the pen and (2) inserting the pen vertically into the cup. In the PileBox task, the demonstration was similarly segmented into two actions: (1) picking up the red box and (2) placing it on top of the green box. We can see that none of these decompositions deviate from human intuition.

A closer examination of the states before and after each segmentation revealed two common features across the tasks:

- Each sub-task began when the robot (released the previous object and) started reaching for the next relevant object.
- Each sub-task ended once the action’s completion was visually confirmed. (In a grasping action, for example, the sub-task did not end when the hand merely contacted the object, but rather when the object was lifted slightly off the table, confirming a successful grasp.)

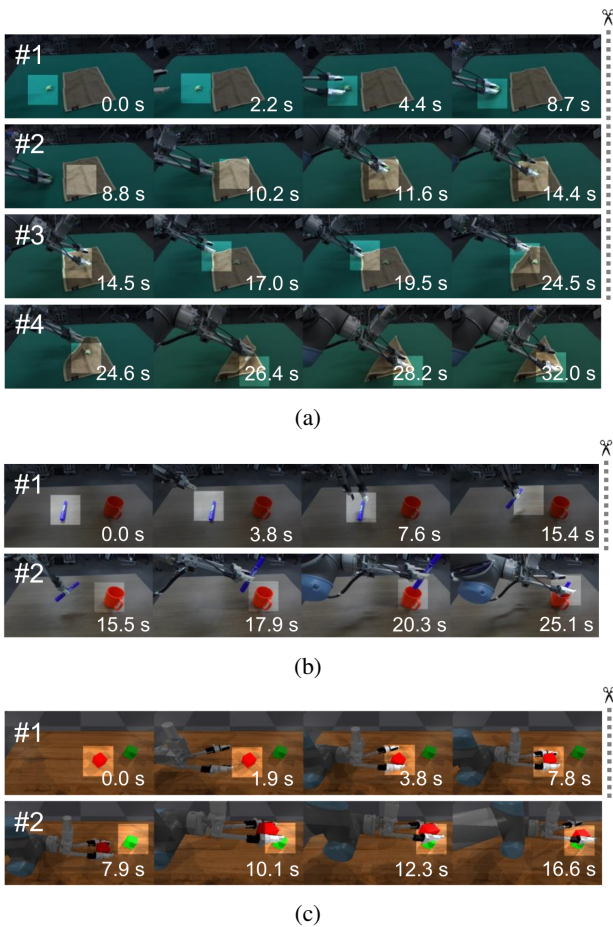


Fig. 2: Typical task decomposition results using the proposed method for the tasks of WrapCandy (a), PenInCup (b), and PileBox (c). The unshaded square areas represent the images cropped around the gaze positions.

D. Consistency of Task Decomposition

In this section, we evaluated the consistency of the resulting task decomposition. Table I shows the number of demonstrations classified as “minority data,” in which the segmentation timings or the number of sub-tasks differed from the most common (majority) decomposition for each task. In addition to the proposed approach, we also evaluated the decomposition consistency under the following ablation settings: (1) without the refinement process (**w/o refine**), (2) detecting changes based solely on the gaze position \hat{g}_t (**w/o feat**), (3) detecting changes based solely on visual features around the gaze f_t (**w/o pos**), and (4) omitting the refinement process from these two settings (**w/o feat, refine** and **w/o pos, refine**).

As illustrated in Table I, we found that all demonstrations across all tasks were segmented in a consistent manner when the refinement process was applied. In contrast, removing the refinement process led to some demonstrations whose decomposition differed from the majority. The number of such minority cases increased noticeably in settings where the gaze position was not used (i.e., w/o pos, refine) com-

TABLE I: Number of minority demonstrations exhibiting task decomposition with different timing or segment counts from the majority in each task.

	WrapCandy	PenInCup	PileBox	Total
Ours	0 / 64	0 / 125	0 / 147	0 / 336
- w/o refine	1	1	3	5
- w/o feat	0	0	0	0
- w/o feat, refine	1	1	3	5
- w/o pos	0	0	0	0
- w/o pos, refine	4	4	45	53

pared to those where it was used (i.e., w/o refine and w/o feat, refine). In each scenario, we observed instances of over-segmentation when the gaze shifted slightly during an action, or missed segmentation when the gaze displacement was too small (e.g., when objects were close together). Furthermore, in the condition where only gaze features were employed, change detection was triggered whenever the end-effector or a grasped object entered the cropped image region, resulting in over-segmentation.

E. Hyperparameter Robustness

Ensuring that the task decomposition results remain consistent despite changes in hyperparameters is critical for the generality and robustness of the proposed method. In this section, we investigate how variations in the hyperparameters $w, b, \theta_{pos}, \theta_{feat}$ used by our method affect the number of correctly segmented demonstrations.

In the previous experiment (Table I), we confirmed that, when gaze position was employed for change detection, the presence or absence of gaze feature data had no significant impact on the segmentation results. Therefore, in this experiment, we performed task decomposition using only the gaze position. Under this condition, the relevant hyperparameters are w and θ_{pos} . Specifically, w determines the filtering strength of the median filter applied to the gaze position, while θ_{pos} determines the sensitivity for detecting gaze transitions.

Fig. 3 shows the number of demonstrations that were correctly segmented when w was set to $\{5, 10, 15, 20, 25, 30\}$ and θ_{pos} was set to $\{25, 50, 75, 100, 125, 150\}$. When hyperparameters varied extensively, the number of demonstrations that resulted in incorrect decomposition exhibited gradual fluctuations in the absence of refinement processing (Fig. 3b). In contrast, with refinement processing applied, decomposition was successfully achieved for all demonstrations across the broad parameter range (Fig. 3b). These findings allow us to conclude that the proposed method possesses the robustness necessary for application to various robotic systems.

In cases where incorrect task decomposition persisted after the refinement process, including instances where the number of successfully segmented demonstrations was lower with refinement (Fig. 3b) than without it (Fig. 3a), decomposition errors resulting from an incorrect number of segments had already become predominant beforehand. Consequently, instead of achieving its intended purpose, the refinement

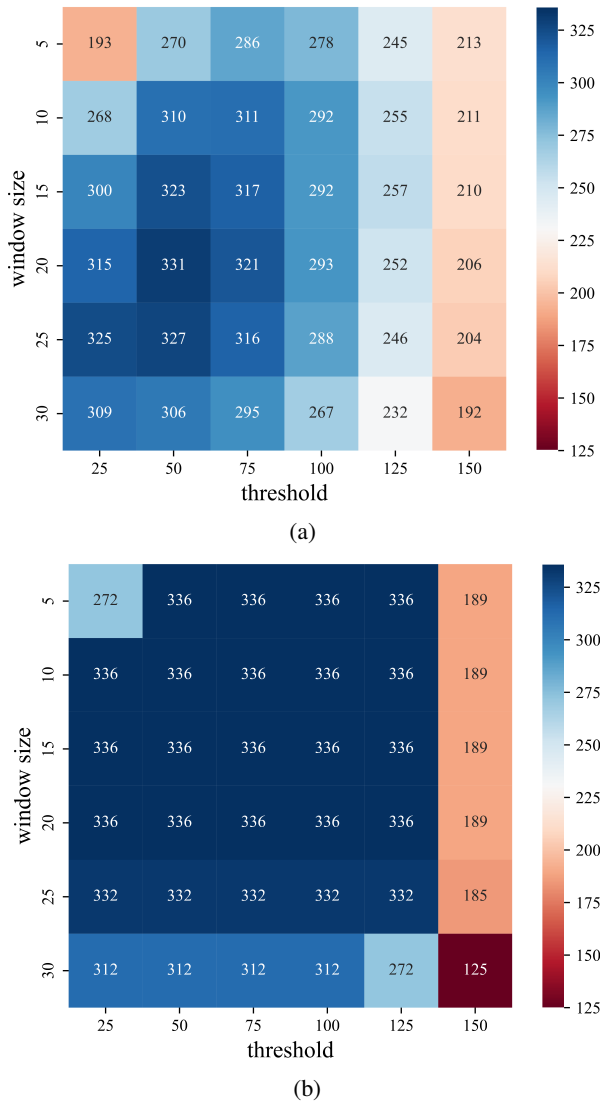


Fig. 3: Number of successfully decomposed demonstrations when varying the hyperparameters. (a) Without refinement process. (b) With refinement process.

process altered demonstrations that had been correctly segmented initially, leading to an incorrect number of sub-tasks. Furthermore, setting the window width w to 25 or higher caused the influence of median filtering to become excessively strong. As a result, it became impossible to detect the required number of segmentation points during the refinement process, regardless of how much the threshold θ_{pos} was lowered.

V. CONCLUSIONS

In this study, we proposed a practical method that provides a consistent and robust task decomposition for robot manipulation in a recent imitation learning framework. The most important finding is that the desired task decomposition was successfully achieved for all demonstrations by adjusting the threshold in the refinement process. This result suggests that utilizing gaze transitions for task decomposition is

fundamentally effective.

However, the proposed method has several limitations. Based on the characteristics of the current imitation learning dataset, we assumed that all demonstrations for a given task consist of the same set of sub-tasks. In contrast, in natural settings, the actions taken to accomplish the same task may consist of a different number of sub-tasks. For example, when pouring water into a cup, one may either grasp the cup before pouring or pour without grasping it. In even more general settings, demonstrations are no longer labeled by task, and a single demonstration may include multiple tasks, as seen in *play data* [31]. In such cases, our gaze transition detection can be performed, but the refinement process cannot be applied, resulting in several percent incorrect task decomposition.

To achieve greater autonomy in the future, robots must be capable of directly observing and imitating human behaviors rather than relying on teleoperation. In such a scenario, the robot can no longer use the expert’s gaze as supervision. Therefore, breakthroughs in autonomous gaze control are urgently needed so that the robot can determine where to focus during the demonstration in an unsupervised manner.

REFERENCES

- [1] H. Kim, Y. Ohmura, and Y. Kuniyoshi, “Goal-conditioned dual-action imitation learning for dexterous robot manipulation,” *IEEE Transactions on Robotics*, vol. 40, pp. 2287–2305, 2024.
- [2] C. Wang, L. J. Fan, J. Sun, R. Zhang, L. Fei-Fei, D. Xu, Y. Zhu, and A. Anandkumar, “Mimicplay: Long-horizon imitation learning by watching human play,” in *Conference on Robot Learning*, 2023.
- [3] K. Black, M. Nakamoto, P. Atreya, H. R. Walke, C. Finn, A. Kumar, and S. Levine, “Zero-shot robotic manipulation with pre-trained image-editing diffusion models,” in *The Twelfth International Conference on Learning Representations*, 2024.
- [4] A. L. Yarbus, “Eye movements and vision,” in *Springer US*, 1967.
- [5] M. Hayhoe and D. Ballard, “Eye movements in natural behavior,” pp. 188–194, 2005.
- [6] M. Land, N. Mennie, and J. Rusted, “The roles of vision and eye movements in the control of activities of daily living,” *Perception*, vol. 28, pp. 1311–1328, 1999.
- [7] M. M. Hayhoe, A. Shrivastava, R. Mruczek, and J. B. Pelz, “Visual memory and motor planning in a natural task,” pp. 49–63, 2003.
- [8] H. Kim, Y. Ohmura, and Y. Kuniyoshi, “Using human gaze to improve robustness against irrelevant objects in robot manipulation tasks,” *IEEE Robotics and Automation Letters*, vol. 5, pp. 4415–4422, 7 2020.
- [9] —, “Gaze-based dual resolution deep imitation learning for high-precision dexterous robot manipulation,” *IEEE Robotics and Automation Letters*, vol. 6, pp. 1630–1637, 4 2021.
- [10] A. Brohan, N. Brown, J. Carbajal, Y. Chebotar, J. Dabis, C. Finn, K. Gopalakrishnan, K. Hausman, A. Herzog, J. Hsu, J. Ibarz, B. Ichter, A. Irpan, T. Jackson, S. Jesmonth, N. J. Joshi, R. Julian, D. Kalashnikov, Y. Kuang, I. Leal, K.-H. Lee, S. Levine, Y. Lu, U. Malla, D. Manjunath, I. Mordatch, O. Nachum, C. Parada, J. Peralta, E. Perez, K. Pertsch, J. Quiambao, K. Rao, M. Ryoo, G. Salazar, P. Sanketi, K. Sayed, J. Singh, S. Sontakke, A. Stone, C. Tan, H. Tran, V. Vanhoucke, S. Vega, Q. Vuong, F. Xia, T. Xiao, P. Xu, S. Xu, T. Yu, and B. Zitkovich, “Rt-1: Robotics transformer for real-world control at scale,” 2023.
- [11] H. Bharadhwaj, J. Vakil, M. Sharma, A. Gupta, S. Tulsiani, and V. Kumar, “Roboagent: Generalization and efficiency in robot manipulation via semantic augmentations and action chunking,” *2024 IEEE International Conference on Robotics and Automation (ICRA)*, pp. 4788–4795, 2023.
- [12] H. Kim, Y. Ohmura, and Y. Kuniyoshi, “Multi-task real-robot data with gaze attention for dual-arm fine manipulation,” *2024 IEEE/RSJ International Conference on Intelligent Robots and Systems (IROS)*, pp. 8516–8523, 2024.

- [13] M. J. Kim, K. Pertsch, S. Karamcheti, T. Xiao, A. Balakrishna, S. Nair, R. Rafailov, E. P. Foster, P. R. Sanketi, Q. Vuong, T. Kollar, B. Burchfiel, R. Tedrake, D. Sadigh, S. Levine, P. Liang, and C. Finn, "OpenVLA: An open-source vision-language-action model," in *8th Annual Conference on Robot Learning*, 2024.
- [14] V. Myers, B. C. Zheng, O. Mees, S. Levine, and K. Fang, "Policy adaptation via language optimization: Decomposing tasks for few-shot imitation," *ArXiv*, vol. abs/2408.16228, 2024.
- [15] A. Gupta, A. Kembhavi, and L. S. Davis, "Observing human-object interactions: Using spatial and functional compatibility for recognition," *IEEE Transactions on Pattern Analysis and Machine Intelligence*, vol. 31, pp. 1775–1789, 2009.
- [16] S. W. Hyder, M. Usama, A. Zafar, M. Naufil, F. J. Fateh, A. Konin, M. Z. Zia, and Q.-H. Tran, "Action segmentation using 2d skeleton heatmaps and multi-modality fusion," *2024 IEEE International Conference on Robotics and Automation (ICRA)*, pp. 1048–1055, 2024.
- [17] C. R. G. Dreher, M. Wächter, and T. Asfour, "Learning object-action relations from bimanual human demonstration using graph networks," *IEEE Robotics and Automation Letters*, vol. 5, pp. 187–194, 2020.
- [18] F. Wörgötter, E. E. Aksoy, N. Krüger, J. Piater, A. Ude, and M. Tamosiunaite, "A simple ontology of manipulation actions based on hand-object relations," *IEEE Transactions on Autonomous Mental Development*, vol. 5, pp. 117–134, 2013.
- [19] C. S. Lea, M. D. Flynn, R. Vidal, A. Reiter, and G. Hager, "Temporal convolutional networks for action segmentation and detection," *2017 IEEE Conference on Computer Vision and Pattern Recognition (CVPR)*, pp. 1003–1012, 2016.
- [20] A. Fathi, A. Farhadi, and J. M. Rehg, "Understanding egocentric activities," *2011 International Conference on Computer Vision*, pp. 407–414, 2011.
- [21] D.-A. Huang, L. Fei-Fei, and J. C. Niebles, "Connectionist temporal modeling for weakly supervised action labeling," in *European Conference on Computer Vision*, 2016.
- [22] Hipiny, H. Ujir, J. L. Minoi, S. F. Juan, M. A. Khairuddin, and M. S. Sunar, "Unsupervised segmentation of action segments in egocentric videos using gaze," in *Proceedings of the 2017 IEEE International Conference on Signal and Image Processing Applications, ICSIPA 2017*. Institute of Electrical and Electronics Engineers Inc., 2017, pp. 351–356.
- [23] A. Fathi, Y. Li, and J. M. Rehg, "Learning to recognize daily actions using gaze," in *European Conference on Computer Vision*, 2012.
- [24] J. Liang, B. Wen, K. E. Bekris, and A. Boularias, "Learning sensorimotor primitives of sequential manipulation tasks from visual demonstrations," *2022 International Conference on Robotics and Automation (ICRA)*, pp. 8591–8597, 2022.
- [25] S. H. Lee, I. H. Suh, S. Calinon, and R. Johansson, "Autonomous framework for segmenting robot trajectories of manipulation task," *Autonomous Robots*, vol. 38, pp. 107–141, 2 2015.
- [26] Y. Zhu, P. Stone, and Y. Zhu, "Bottom-up skill discovery from unsegmented demonstrations for long-horizon robot manipulation," *IEEE Robotics and Automation Letters*, vol. 7, pp. 4126–4133, 4 2022.
- [27] S. Nair, A. Rajeswaran, V. Kumar, C. Finn, and A. Gupta, "R3m: A universal visual representation for robot manipulation," in *Conference on Robot Learning*, 2022.
- [28] Z. Zhang, Y. Li, O. Bastani, A. Gupta, D. Jayaraman, Y. J. Ma, and L. Weihs, "Universal visual decomposer: Long-horizon manipulation made easy," *2024 IEEE International Conference on Robotics and Automation (ICRA)*, pp. 6973–6980, 2023.
- [29] A. Radford, J. W. Kim, C. Hallacy, A. Ramesh, G. Goh, S. Agarwal, G. Sastry, A. Askell, P. Mishkin, J. Clark, G. Krueger, and I. Sutskever, "Learning transferable visual models from natural language supervision," in *International Conference on Machine Learning*, 2021.
- [30] S. Hamano, H. Kim, Y. Ohmura, and Y. Kuniyoshi, "Using human gaze in few-shot imitation learning for robot manipulation," *2022 IEEE/RSJ International Conference on Intelligent Robots and Systems (IROS)*, pp. 8622–8629, 2022.
- [31] C. Lynch, M. Khansari, T. Xiao, V. Kumar, J. Tompson, S. Levine, and P. Sermanet, "Learning latent plans from play," in *Conference on Robot Learning*, 2019.